THE ROLE OF BI-MODAL AND LAMELLAR MICROSTRUCTURES OF Ti-6Al-4V ON THE BEHAVIOR OF FATIGUE CRACKS EMANATING FROM EDGE-NOTCHES

M. Benedetti, V. Fontanari
Department of Materials Engineering and Industrial Technologies, University of Trento
Via Mesiano 77, 38050 Trento, Italy. E-mail: matteo.benedetti@ing.unitn.it

Abstract

This paper is aimed at evaluating the influence of bi-modal and lamellar microstructure on the behaviour of small cracks emanating from notches in the α+β titanium Ti-6Al-4V alloy. Pulsating four points bending tests were performed on double-edge-notched specimens. The conditions of initiation and early propagation of fatigue cracks were investigated at two nominal stress levels. Crack closure effects were measured by extensometric technique. The effect of the yielded region at the notch tip, calculated by elastic-plastic finite element modelling of the fatigue tests, was included in the discussion of experimental results. The importance of the bi-modal and lamellar microstructure on the material damage was correlated to the observed oscillations in the crack growth rate and compared with long crack propagation data measured using C(T) specimens.

Introduction

A matter of major importance for fatigue life assessment is the understanding of the small crack behaviour at notches, frequently responsible for fatigue crack initiation in aircraft structures, where titanium alloys are mostly used. Due to high applied loads, non-uniform stress fields are developed in the vicinity of notches. It is therefore very important to investigate the growth behaviour of these short fatigue cracks considering notch plasticity effects. In a recent investigation on the behaviour of small fatigue cracks emanating from notches in Ti-6Al-4V [1], anomalously high growth rates were observed during the early propagation stage and imputed to the so-called notch-plasticity contribution to the driving force for crack advance. Furthermore, crack growth oscillations, observed during the subsequent crack propagation stage beyond the notch plastic zone, were correlated to the maximum dislocation slip length, strongly influenced by the microstructure. Accordingly, two-phase α+β titanium alloys are typically processed in two microstructural conditions with different α colony size [2]. Coarse grained, so-called lamellar microstructures with large β grains (about 600 μm) and a lamellar matrix of alternating α and β plates can be produced by heat treatment in the high-temperature β-phase field and subsequent slow cooling into the α+β phase-field. So-called bi-modal microstructures can be produced by recrystallization in the α+β phase-field and consist of primary α grains (volume fraction about 30 to 60 pct, grain size ~ 20 μm) with a colony-type lamellar matrix of alternating α and β plates within small β grains (20 to 40 μm).

Starting from these outcomes, the present work is focused on the not fully developed questions previously arisen, such as the influence of slip length (i.e. of the microstructure) as well as the effect of crack closure on the small crack behaviour. To this purpose, pulsating four point bending tests were performed on double-edge-notched specimens with both bi-

modal and lamellar microstructure. The conditions of initiation and early propagation of fatigue cracks were investigated through microscopic observation of the specimen surface and post-fracture fractographic analysis. Stress redistribution due to notch plasticity was evaluated by means of finite element modelling. Crack closure effects were considered for correcting the effective stress intensity factor range. Crack growth rate data were correlated by linear elastic fracture mechanics and compared with those measured using standard C(T) specimens (long crack).

Material and experimental procedure

The Ti-6Al-4V alloy (Ti-5.9Al-4.1V-0.1Fe, wt.-%) was supplied by the Italian Titanium Development Centre in form of a rolled bar stock. The specimens were solution treated at 955°C for 1 hour (to adjust a volume fraction of about 60% primary α grains), followed by controlled cooling (50 °C/min) to room temperature and then stress relieved (700°C for 2 h). The resulting microstructure, shown in Fig. 1a, consisted of a bi-modal distribution of interconnected equiaxed primary α grains and lamellar α+β colonies (transformed β); the average grain size obtained was ~20 μm. A fully lamellar Ti-6Al-4V structure was also examined. This microstructure (Fig. 1b) was obtained by solution treating at 1050°C for 1 hour, followed by controlled cooling from the β single phase field to room temperature (25 °C/min) and then stress relieved (700°C for 2 h). The resulting microstructure had an average prior-β grain of ~1 mm, a colony size (parallel-oriented α-phase lamellae) of 500 μm, and an average α lamellae lath width of ~2 μm, similar to the interlamellar spacing of the transformed β in the bi-modal microstructure.

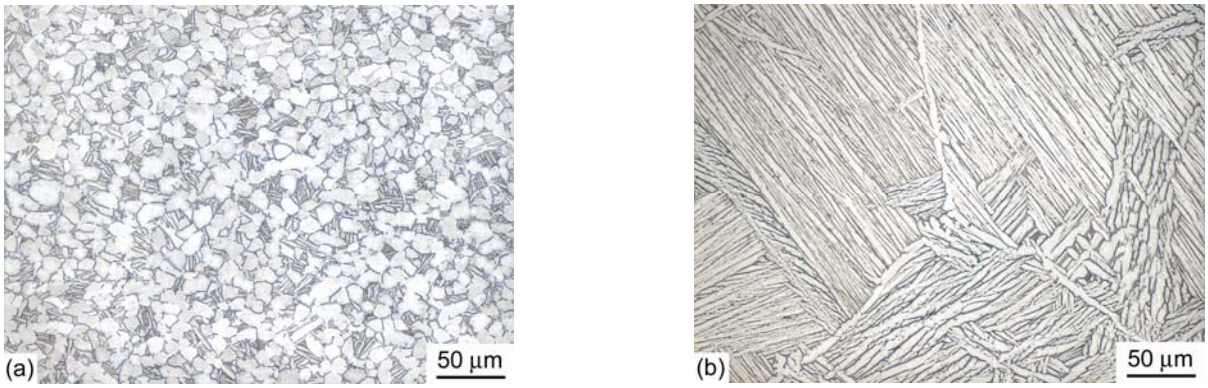

FIGURE 1. Ti-6Al-4V: (a) bi-modal and (b) lamellar microstructure.

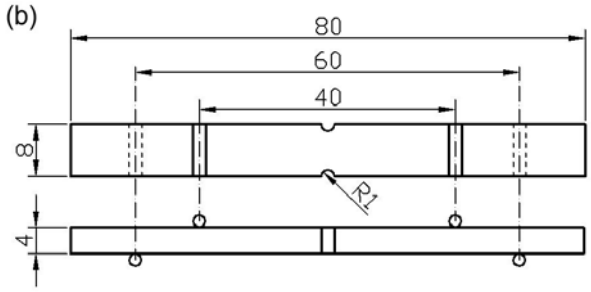

FIGURE 2. Four point bending fatigue test configuration (dimensions in mm).

To evaluate the cyclic stress-strain behaviour, reverse strain axial testing was performed on plain hourglass specimens by multiple-step test. Fatigue characterization was carried out on double-edge-notched specimens (Fig. 2), selected in order to monitor the propagation of quarter-elliptical corner cracks along both axes (i.e., along specimen width and thickness)

thus allowing a more precise ΔK calculation taking into account the changes in crack aspect ratio. Four-point bending fatigue tests were carried out providing for a theoretical elastic stress concentration factor of 1.82. A sinusoidal pulsating (stress ratio R=0.1) load waveform was applied at a frequency of 15 Hz. In order to study the effect of stress amplitude on small fatigue crack propagation, the experimentation was performed at two different stress levels: the first one corresponding to a nominal maximum stress S_{max} of 750 MPa, the second one to S_{max} of 500 MPa, respectively. Because of the notch effect, the local stress conditions for both applied stress levels were above the yield stress of the material (~850 MPa). Measurements of crack closure were obtained by using the back face strain gauge technique. Small strain gauges with grid size of 0.2 mm were bonded at the notch root to the upper specimen surface to detect the strain variation produced by the closure or opening of the underlying crack.

Results and discussion

Stress field analysis

The monotonic and cyclic stress-strain response of both microstructures are compared in Fig. 3. Both microstructural conditions exhibited a cyclic yield strength somewhat higher than the monotonic value: 850 vs. 840 MPa for the bi-modal, 870 vs. 850 MPa for the lamellar microstructure. The bi-modal condition displayed a significant cyclic strain hardening rate, whereas the lamellar microstructure showed a slight softening tendency so that at strain amplitudes higher than 0.014 the cyclic curve cross cut the monotonic curve.

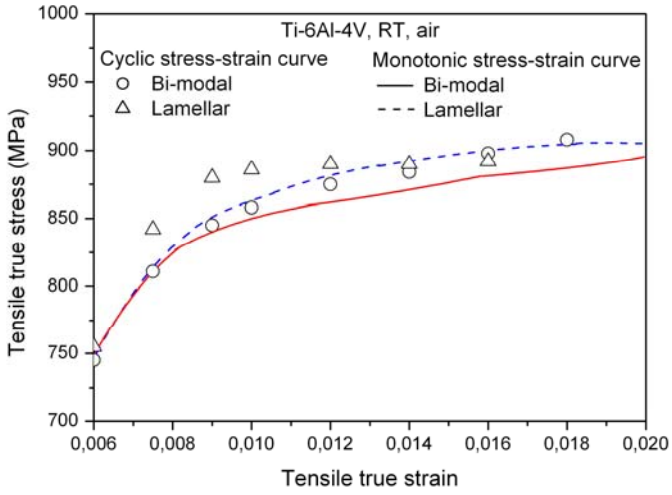

FIGURE 3. Ti-6Al-4V. Cyclic and monotonic stress-strain curves.

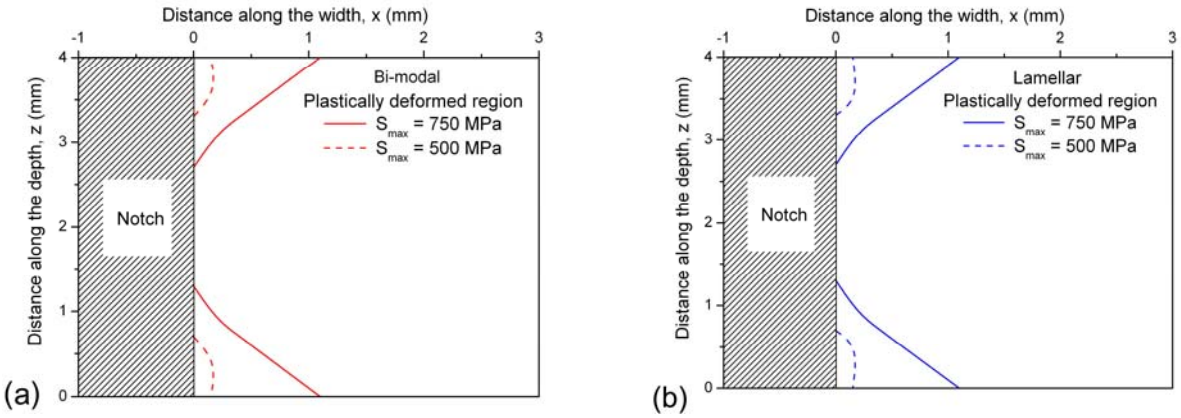

FIGURE 4. Extension of the notch plastic zone. (a) bi-modal, (b) lamellar microstructures.

The cyclic stress redistribution was assessed by finite element modelling using the Lemaitre-Chaboche criterion to represent the cyclic material behaviour. The first three stress-strain cycles were modeled, showing that the plastic deformation spread from the notch tip in the first loading ramp (monotonic plasticity), followed by elastic stabilisation owing to the cyclic strain hardening displayed by both microstructures. Noteworthy, despite the positive value of the nominal stress ratio, a region developed close to the notch root, where the local stress ratio is negative. The region experiencing monotonic plastic deformation is shown in Figs. 4a and 4b for the bi-modal and lamellar microstructures, respectively. At the higher stress level the notch plastic zone spreads over 1.1 mm along the specimen-width and over 1.4 mm along the specimen-depth, whereas at the lower stress level it is confined to about 200 μm around the notch. In order to evaluate the effect of the stress redistribution at notch root on the initiation of fatigue cracks, the equivalent stress amplitude and hydrostatic mean stress expressed according to the Sines formulation were evaluated at each node of the FE mesh. The critical stress conditions for crack initiation were identified, for both microstructures as well as for both stress levels, on the notch surface between the notch edge and nearly 100 μm underneath. Accordingly, a volume is "critically" stressed at the notch root, where fatigue cracks may initiate in the weakest microstructural constituent [3].

Fatigue crack behavior

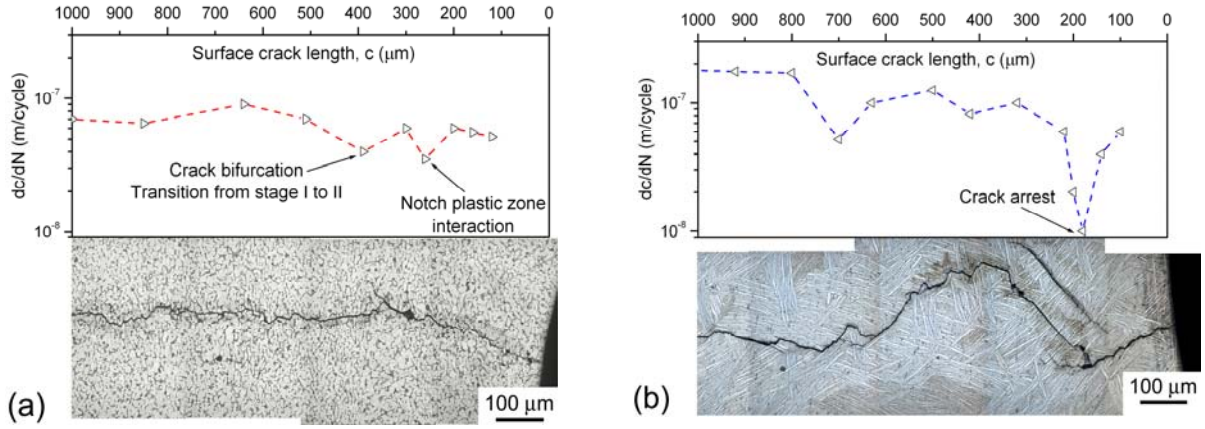

FIGURE 5. Typical crack path profile observed for the (a) bi-modal and (b) lamellar microstructure in the notch region.

Involvement of mixed mode (stage I) was observed during the early stage of fatigue crack growth (up to ~400 μm surface crack length), as confirmed also by crack profiles taken in the notch region and represented in Figs. 5a-b for the bi-modal and the lamellar microstructures, respectively. This observation suggests that shear mode relative displacement within the notch plastic zone is responsible for crack advance [4]. In the bi-modal microstructure, the transition from stage I to stage II was accompanied by crack bifurcation. This means that two competitive crack growth mechanisms, i.e. shear and opening modes, were operative; at length of about 400 μm, the crack reached enough driving force to propagate in mode I, whereas the crack branch, propagating in mixed mode, stopped growing. In the lamellar microstructure, transgranular stage I involved crystallographic crack propagation favoured by aligned α lamellar colonies. If the main axes of the lamellae were oriented more or less parallel to the load axis, the crack cut directly across the lamellae (perpendicular to their surface). If the lamellae were aligned roughly perpendicular to the load axis, the crack grew along the lamellae boundaries [5]. The subsequent mode I (stage II) crack propagation followed a more tortuous and deflected crack path in the lamellar compared to the bi-modal

microstructure. The high degree of tortuosity and crack bifurcation was a result of the interactions of the crack with relatively coarse microstructure (colony size of ~500 μm). The local crack path in the bi-modal material was also somewhat influenced by the microstructure, but the resulting tortuosity is significantly lower, consistent with the magnitude of finer microstructural size scales (grain size of ~20 μm). Furthermore, the crack path in the bi-modal structure resulted in both inter- and transgranular crack propagation.

The relation between crack growth rate and surface crack length for the bi-modal microstructure at the lower load level is plotted in Fig. 6a. The crack growth rates step down to the lowest value when the crack length is about 250 μm, at the extremity of the notch plastic zone. This minimum value in the curve characterizes the 'abnormal' behaviour of small cracks emanating from notches since the early crack propagation stage is dictated by the notch plasticity [6]. Fig. 5a compares the crack path with the measured crack growth rates. A slight decrement in crack growth rate is attained at the transition from stage I to stage II. Subsequently, small oscillations in crack propagation rate are observed up to ~1 mm crack length. These were induced by local interactions of the crack-tip plastic zone with microstructural barriers to plastic flow, as ob-served previously. Such oscillations occurred in a crack length interval of about 150 μm. This suggests that the microstructural feature controlling small crack growth at this load level were the interconnecting globular primary α grain [2], having the same size of the crack growth oscillation intervals. Comparable crack growth rates are displayed by the lamellar microstructure (Fig. 6b), which is, however, characterized by a more pronounced microstructure-sensitivity. Small cracks exhibited noticeable intermittent acceleration and deceleration and even crack arrest, presumably due to the crack tip encountering transitory obstacles like β grain boundaries or other adverse crack growth mechanisms, i.e. lamellae unfavourably oriented towards the load axis. Particularly unfavourable, eventually causing the crack to arrest, seem to be the lamellae aligned parallel to the load axis, as illustrated by Fig. 5b comparing the crack path with the measured crack growth rates. The crack kept on displaying such erratic growth up to ~2 mm crack length. Straight crack path to cut across parallel-aligned lamellae is associated by higher crack growth rates. The observed fluctuations in crack growth rate for the lamellar material point out that the near-tip microstructure can be the primary factor governing crack growth for extension over length scales comparable to microstructural dimensions. The heterogeneous crack growth resistance, characteristic of lamellar Ti-6Al-4V, contributed significantly to the strong influence of microstructure on the local crack path in this material. On the other hand, the bi-modal Ti-6Al-4V exhibited more homogeneous crack-growth resistance. In fact, the influence of the near-tip microstructure on crack growth behaviour occurred over much smaller length scales (i.e. the size of the interconnecting primary α grains) and, with reduced effects (i.e. smaller crack growth rate fluctuations). Fig. 6c shows the crack growth rates versus the surface crack length for the bi-modal structure at the higher stress level. In this case, the effect of notch plasticity on fatigue crack behaviour is particularly emphasized. The driving force for crack propagation is mostly given by the notch contribution (mechanically small crack). Consequently, the crack growth rate is high after initiation, remaining approximately constant with increasing crack length and exhibiting a minimum value at about 500 μm surface crack length. As schematized by the model illustrated in Ref. 1, the minimum crack growth rate was attained at the boundary of the notch plastic zone. Similar behaviour was displayed by the lamellar microstructure (Fig. 6d), which is, however, characterized by a more pronounced microstructure-sensitivity [2]. In fact, crack growth rate fluctuations and, sometimes, crack arrests were observed even in the notch plastic zone, although a tendency to a minimum crack growth rate at about 500 μm crack length is evident. Such behaviour should be caused by a non-uniform distribution of the plastic strain around the notch because of the

heterogonous coarse lamellar microstructure. Lamellar colonies unfavourably oriented towards the load axis did not experience plastic deformation, thus hindering further crack extension.

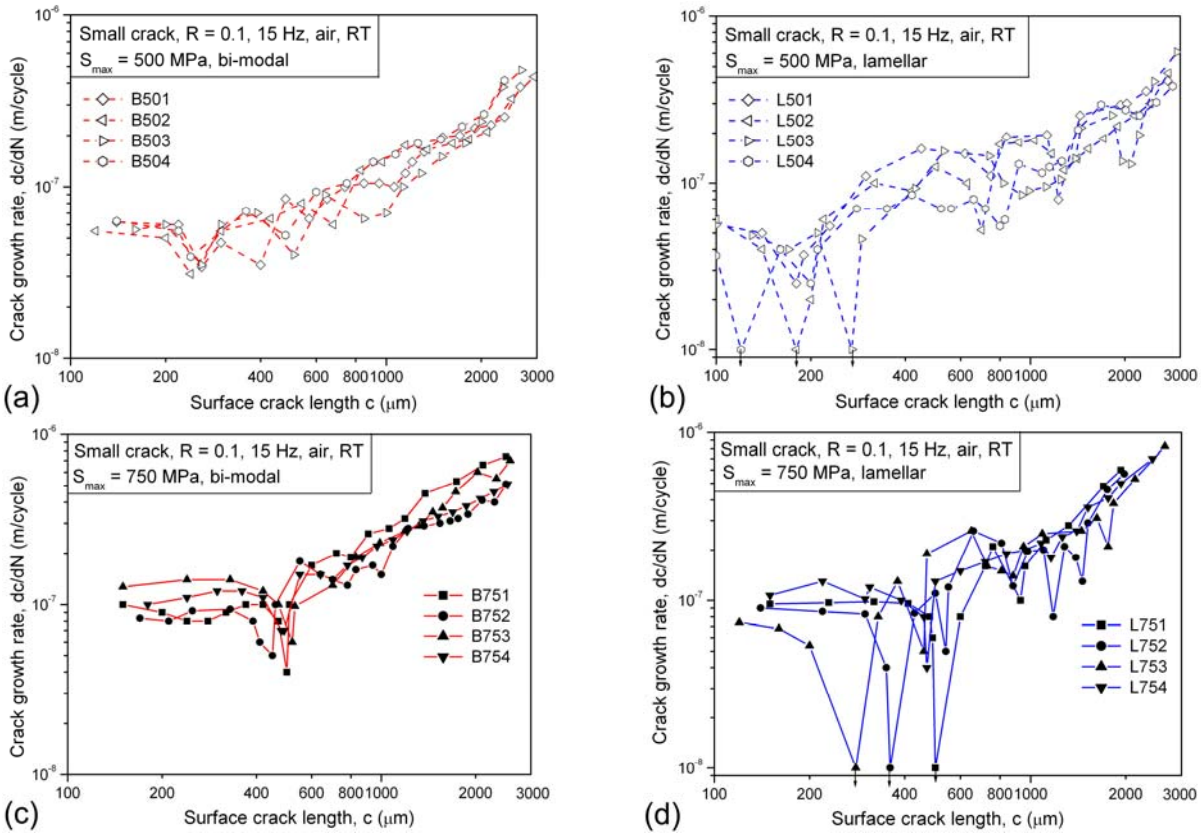

FIGURE 6. Fatigue crack growth rates plotted vs. surface crack length. (a) and (c) bi-modal (circular symbols), (b) and (d) lamellar microstructures (triangular symbols). (a) and (b) S_{max} = 500 MPa, (c) and (d) S_{max} = 750 MPa. The symbols "↓" indicate crack arrest.

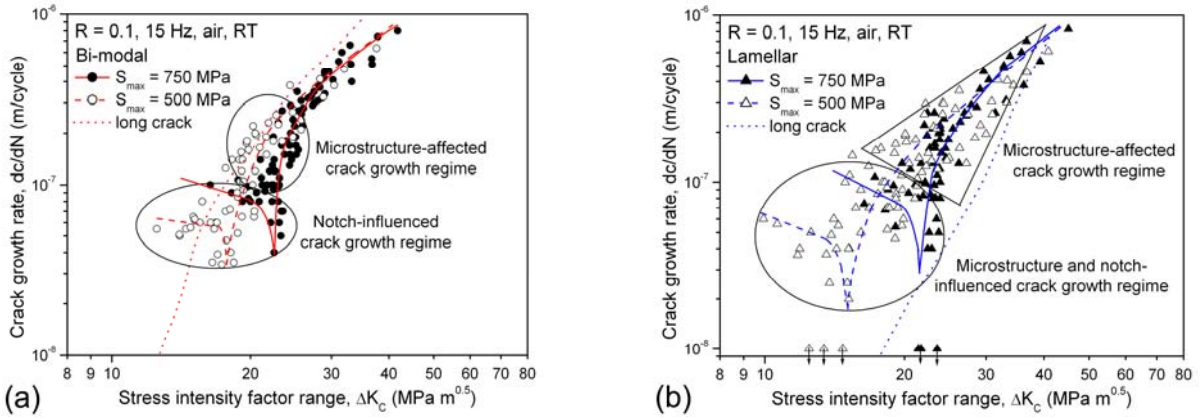

FIGURE 7. Fatigue crack growth rates plotted vs. ΔK.

In order to represent crack growth rates as a function of a fracture mechanics parameter, the stress intensity factor was calculated using an appropriate weight function [7]. In Figures 7a and 7b the crack growth rates for both load levels are plotted versus the stress intensity factor range for the bi-modal and lamellar microstructures, respectively, and compared with long crack data. These data were measured using standard C(T) specimens with same microstructural conditions. Details regarding experimental procedures are provided in Ref. 8. Unlike long crack growth data, there is little difference in the resistance of the two

microstructures to small-crack propagation. When the crack size is comparable to the characteristic microstructural dimension, the material inherent fracture properties are only dictated by the maximum dislocation slip length [2]. Accordingly, the inherent propagation mechanism along planar slip bands is very fast in coarse colony-type lamellar microstructures because of the much longer slip length, compared to finer scaled microstructures [2]. The anomalous behaviour of small crack emanating from notches is evident in Figs. 7a-b. In particular, initial crack growth rates were higher than expected, being the driving force for crack propagation not only given by crack tip plasticity but also by notch plasticity: the wider the notch plastic zone, the higher crack growth rates [8]. As the crack had overcome the notch plastic zone, the microstructural influence on crack growth was still present, especially at the lower load level, and died out upon reaching the long-crack regime, where data referring both to higher and lower load levels tended to gather. Unexpectedly, for the bi-modal microstructure, microstructurally small cracks, especially at the lower load level, grew slower than long cracks at the same ΔK level. Conversely, the lamellar microstructure showed considerably more scattered crack growth rates due to crack-tip interactions with the coarser lamellar microstructure, even within the notch plastic zone.

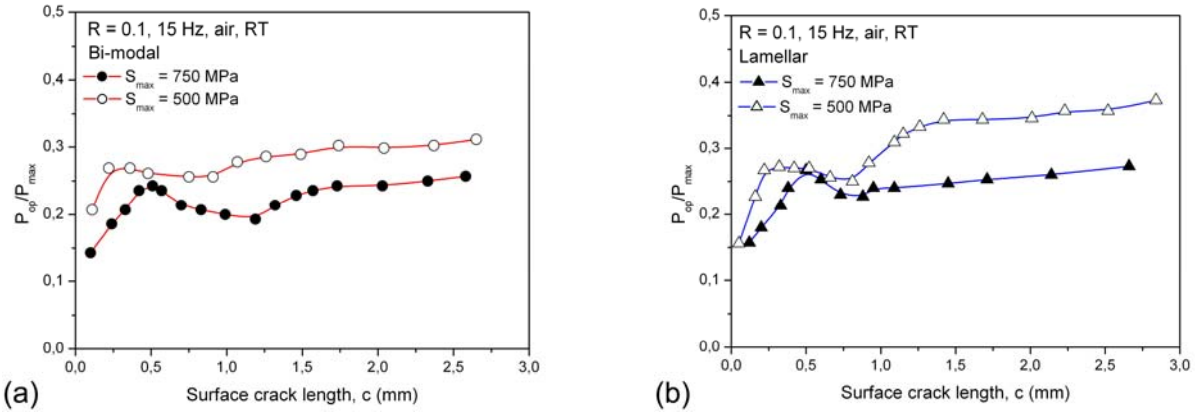

FIGURE 8. Variation of relative opening load with surface crack length.

In order to account for the anomalous behaviour of the small cracks emanating from notches, crack closure effect was investigated. The relation between the opening load ratio and the surface crack length is plotted in Figs. 8a-b for the bi-modal and lamellar microstructures, respectively. The closure load was small (P_{op} / P_{max} ~0.15) at the very beginning and increased with crack length until a maximum value was reached at the extremity of the notch plastic zone, then it decreased until the crack grew to ~1 mm. Finally, the closure load grew slowly with increasing crack length. Because of the stress concentration at the notch, the plastic deformation took place in the root area and was associated with a volume expansion inducing a closure effect even for a small crack wake ('geometry' induced crack closure [3]). Beyond the notch plastic zone, the plastic deformation was negligible, thus causing the opening load to decrease slightly. When the crack wake became large enough, the opening force increased again, resulting from a combination of surface roughness and shear displacement (mode II) at the tip of the crack ('surface roughness' induced crack closure [9]), particularly evident for the lamellar microstructure owing to the increased tortuosity in the crack path and, hence, in the fracture-surface roughness. From the above discussion it is clear that the closure effect should be considered when fatigue crack propagation at a notch root is described. Therefore, the crack growth rates are plotted vs. the calculated stress intensity factor range, corrected for crack closure, in Figs 9a-b for the bi-modal and lamellar microstructures, respectively. The curves show a fairly good rationalization of the data. In particular, the data regarding the bi-modal microstructure merge with the results of long crack

propagation measured using standard C(T) specimens, especially when the crack becomes microstructurally long, i.e. 8 times longer than the characteristic microstructural dimension, which is the size of interconnecting primary α-grains [2]. This observation proves that additional 'notch-induced' crack closure effect should be considered for cracks emanating from stress concentration features. Data regarding the lamellar microstructure resulted in higher propagation rates of small cracks compared to the bi-modal microstructure as a consequence of the larger colony size resulting in a longer slip length. Furthermore, small cracks grew faster than long cracks, even correcting the stress intensity factor range for crack closure effects. This fact indicates that the studied cracks were microstructurally small even in the late propagation stage because of the coarse lamellar microstructure. In fact, their superior resistance to the propagation of long cracks compared to small cracks is imputed not only to crack closure effects, but also to other extrinsic secondary effects, such as rough crack front geometry and crack bridging [10]. Accordingly, when all extrinsic crack growth retardation mechanisms are effective, small and long crack growth rate data tend to merge together. Noteworthy, specimens displaying small crack growth rates comparable to those of long cracks showed some evidences of crack bridges, i.e. unbroken ligaments behind the crack front, which contributed to transfer part of the applied load and therefore reduced the applied driving force for fatigue crack extension.

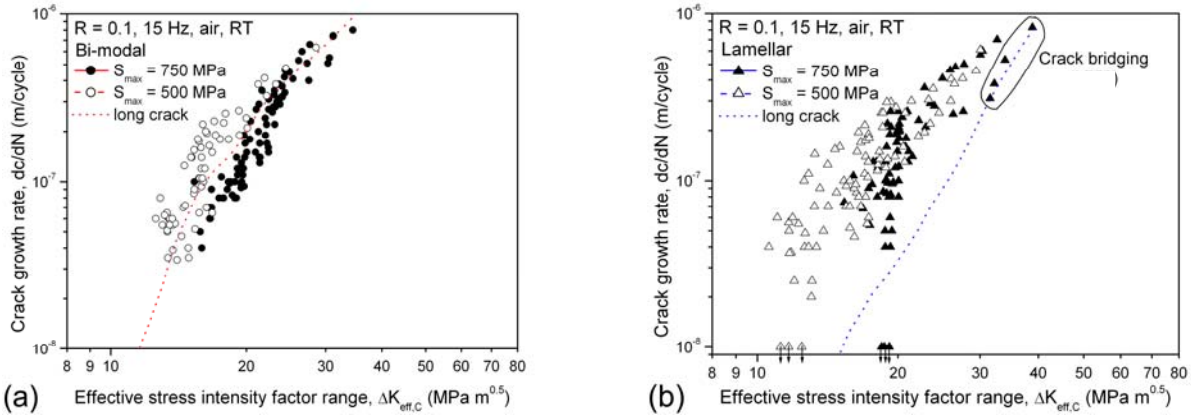

FIGURE 9. Fatigue crack growth rates plotted vs. ΔK corrected for crack closure.

References

1. Benedetti, M., Bertini, L., Fontanari, V., *Fatigue Fract Engng Mater Struct*, vol. 27, 111-125, 2004.
2. Lütjering, G., Williams, J. C., *Titanium*, Springer, Berlin, Germany, 2003.
3. Evans, W. *J., Mater. Sci. Engng.*, vol. A263, 160-175, 1999.
4. Hammouda, M. M., Smith, R. A., Miller, K. J., *Fatigue Fract Engng Mater Struct*, vol. 2, 139-154, 1979.
5. Langou, M. A., Stock, S. R., *Metall. Mat. Trans.*, vol. 32A, 2315-2324, 2001.
6. Zhao, W., Wu, X. R., *Fatigue Fract Engng Mater Struct*, vol. 13, 347-360, 1990.
7. Heidemann, J., Benedetti, M., Peters, J.O., Lütjering, G., In *Proceedings of the 10th World Conference on Titanium*, edited by G. Lütjering, Wiley-VCH, Weinheim, 2003.
8. Rosenberg, G., *Fatigue Fract Engng Mater Struct,* vol. 21, 727-739, 1998.
9. James, M. R., Morris, W. L., *Metall. Mat. Trans.*, vol. 14A, 153-158, 1983.

10. Ritchie, R. O., *Int. J. Fracture*, vol. **100**, 55-83, 1999.